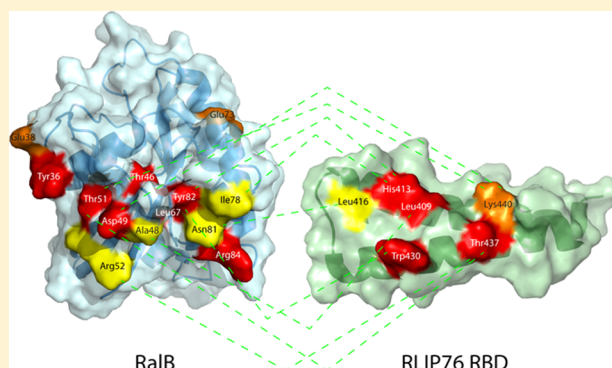


# Thermodynamic Mapping of Effector Protein Interfaces with RalA and RalB

Louise J. Campbell, Maria Peppas, Michael D. Crabtree, Arooj Shafiq, Nicholas F. McGough, Helen R. Mott,\* and Darerca Owen\*

Department of Biochemistry, University of Cambridge, 80 Tennis Court Road, Cambridge CB2 1GA, U.K.

**ABSTRACT:** RalA and RalB are members of the Ras family of small G proteins and are activated downstream of Ras via RalGEFs. The RalGEF-Ral axis represents one of the major effector pathways controlled by Ras and as such is an important pharmacological target. RalA and RalB are approximately 80% identical at the amino acid level; despite this, they have distinct roles both in normal cells and in the disease state. We have used our structure of RalB-RLIP76 to guide an analysis of Ral-effector interaction interfaces, creating panels of mutant proteins to probe the energetics of these interactions. The data provide a physical mechanism that underpins the effector selective mutations commonly employed to dissect Ral G protein function. Comparing the energetic landscape of the RalB-RLIP76 and RalB-Sec5 complexes reveals mutations in RalB that lead to differential binding of the two effector proteins. A panel of RLIP76 mutants was used to probe the interaction between RLIP76 and RalA and -B. Despite 100% sequence identity in the RalA and -B contact residues with RLIP76, differences still exist in the energetic profiles of the two complexes. Therefore, we have revealed properties that may account for some of the functional separation observed with RalA and RalB at the cellular level. Our mutations, in both the Ral isoforms and RLIP76, provide new tools that can be employed to parse the complex biology of Ral G protein signaling networks. The combination of these thermodynamic and structural data can also guide efforts to ablate RalA and -B activity with small molecules and peptides.



The Ral proteins are small G proteins that are activated downstream of Ras. There are two human Ral proteins, RalA and RalB, that despite being 82% identical at the amino acid level have distinct cellular functions. Both proteins have roles in the regulation of cytokinesis. RalA acts first to secure the exocyst complex to the cytokinetic furrow; this is followed by RalB activity, which engages the exocyst at the midbody of the cytoplasmic bridge to drive abscission.<sup>1</sup> RalB has been demonstrated to promote autophagocytosis,<sup>2</sup> while RalA controls mitochondrial fission at mitosis.<sup>3</sup> Both Ral proteins also have roles in targeted exocytosis, receptor-mediated endocytosis, and the regulation of the actin cytoskeleton, and while individual roles have not been assigned to RalA and RalB in these processes, it seems likely they will emerge. In fact, some specific roles are already known; for example, RalA drives polarized exocytosis in epithelial cells,<sup>4</sup> whereas RalB controls exocytosis during polarized cell migration.<sup>5</sup> Distinctive roles have also been assigned to RalA and RalB in the disease state: RalA is required for anchorage-independent proliferation in cancer cell lines, while RalB is necessary for tumor cells to avoid apoptosis.<sup>6</sup>

Like most other small G proteins, the Ral proteins are found in two forms. When bound to GDP, they are inactive, but when bound to GTP, they adopt their active conformation and can engage with downstream effector proteins, initiate signaling cascades, and control cellular outcomes. The functional

individuality of RalA and RalB is even more surprising considering they interact with the same set of downstream effector proteins and therefore share control of the same collection of signaling pathways.<sup>7</sup> Proposals for the mechanism underlying the specific actions of the Ral proteins in the absence of differential sets of effector proteins include distinctive cellular localization and divergent activation. The active conformation of small G proteins is based around two regions of the protein, known as switch 1 and switch 2, which are sensitive to the presence of the terminal phosphate in GTP. These switch regions mediate the majority of contacts with the effector proteins. RalA and RalB are identical in the switch regions, and most of the variation between the two proteins lies at their C-termini, beyond the structured G domain, in the residues that comprise the “hypervariable region”.<sup>8</sup> In most small G proteins, this region controls membrane localization.<sup>9</sup> Both proteins have been observed localized at the plasma membrane and also at endomembranes. RalA and RalB are geranylgeranylated at Cys203, which constitutes the primary membrane attachment cue, and both contain multiple positively charged side chains preceding this that could act as secondary membrane localization

**Received:** December 17, 2014

**Revised:** January 26, 2015

**Published:** January 26, 2015

signals. Both proteins also carry phosphorylation sites in this region. RalA is phosphorylated at Ser183 and Ser194: pSer194 is a consequence of Aurora A activity and results in translocation of RalA to mitochondria.<sup>3</sup> RalB is phosphorylated by PKC on Ser198; the outcome of this is relocation to endomembranes.<sup>10</sup> Specific membrane localization could result in the Ral proteins encountering subsets of effector proteins and therefore activating specific signaling pathways. Likewise, specificity could also come via distinct actuation signals and activators. Ral proteins are activated by RalGEFs, some of which provide the direct link to Ras signaling. However, there are currently six GEFs that have been identified for the Ral proteins.<sup>7</sup> In the case of cytokinesis, the distinct roles for RalA and RalB are designated by individual pairs of RalGEFs, which coordinate several input signals.<sup>1</sup>

Several effector proteins have been identified for RalA and RalB. The first one to be identified was RLIP76 (also known as RalBP1 and RIP1<sup>11–13</sup>). RLIP76 appears to play multiple, disparate roles in Ral signaling.<sup>7</sup> Alongside RLIP76, two components of the exocyst complex, Sec5 and Exo84, are the best-characterized effector proteins for the Ral proteins. Through these effectors, the Ral proteins control polarized exocytosis<sup>14</sup> but also non-exocyst functions, including activation of TBK1<sup>15</sup> and autophagosome assembly.<sup>2</sup> Ral proteins are also known to interact with ZONAB, a transcription regulator,<sup>16</sup> and filamin, the actin cross-linking protein.<sup>17</sup> Interestingly, the Ral proteins also seem to interact with phospholipase D and phospholipase C- $\delta$ 1 but in a nucleotide-independent manner.<sup>18,19</sup> The latter four interactions are not as well characterized. There is some evidence that RalA and RalB do have differential affinity for their effector proteins,<sup>4</sup> and this would certainly contribute to conferring specific cellular roles to the proteins.

We have previously determined the structure of the complex that forms between RalB and the RLIP76 RBD.<sup>20</sup> We have now used this structure to design mutants of both RalB and RLIP76 to elucidate the thermodynamics of the binding interface produced by the two proteins interacting. In addition, we have used the panel of RalB mutants that we generated to probe the interaction between RalB and a second effector protein, Sec5. Comparing the energetic landscape of the two complexes has revealed mutations in RalB that lead to differential binding of the two effector proteins. We have also used the RLIP76 mutants to probe the interaction between RLIP76 and RalA to compare the energetics of the RalA and RalB complexes. Despite the RalA and -B contact residues for RLIP76 being 100% identical, differences still exist in the energetic profiles of the two complexes.

## METHODS

**Protein Expression Constructs.** Simian RalA  $\Delta$ C (residues 1–184) was amplified by polymerase chain reaction (PCR) and cloned into pMAT10 (D. Owen, unpublished) using *Bam*HI and *Eco*RI sites that had been incorporated into the PCR primers. The resulting construct expresses RalA as an N-terminal His-MBP fusion protein with a thrombin cleavable tag. Full-length Simian RalA (residues 1–206) was amplified by PCR and cloned into pGEX-6P (GE Healthcare) using *Bam*HI and *Eco*RI sites that had been incorporated into the PCR primers. RalB  $\Delta$ C (residues 1–185) was cloned into pET16b using *Nde*I and *Bam*HI sites that had been incorporated into the PCR primers. Full-length human RalB (residues 1–206) was amplified by PCR and cloned into pMAT10P (D. Owen, unpublished) using *Bam*HI and *Eco*RI sites that had been

incorporated into the PCR primers. The resulting construct expresses RalB as an N-terminal His-MBP fusion protein with the tag cleavable using PreScission protease. All Ral expression constructs incorporate the activating mutation Q72L and were expressed in *Escherichia coli* BL21(DE3) (Invitrogen).

The RBD of human RLIP76 (residues 393–446) was cloned into a modified version of pGEX-His-2.<sup>21</sup> A thrombin cleavage site was engineered into pGEX-His-2, 5' to the *Bam*HI cloning site. RLIP76 (residues 393–446) was amplified by PCR and cloned into modified pGEX-His-2 using *Bam*HI and *Xho*I restriction sites that had been incorporated into the PCR primers. The resulting construct expressed GST-RLIP76 RBD with a C-terminal His tag. The C411S mutation was introduced as described below. The construct was expressed in *E. coli* BL21 (Invitrogen). The Sec5 RBD expression construct has been described previously.<sup>22</sup>

**Recombinant Protein Production.** A stationary culture containing pMAT10-RalA  $\Delta$ C was diluted 1:10 into 2TY, grown to an  $A_{600}$  of  $\sim$ 0.8 at 37 °C, induced with 1 mM IPTG, and grown for a further 16 h at 20 °C. Cells were lysed, and the fusion protein was purified using Ni-NTA resin (Qiagen) following the manufacturer's instructions. The fusion protein was cleaved with thrombin to remove the His-MBP tag. A stationary culture containing pGEX-6P-full-length RalA was diluted 1:10 into 2TY, grown to an  $A_{600}$  of  $\sim$ 0.8 at 37 °C, induced with 0.1 mM IPTG, and grown for a further 5 h at 37 °C. Cells were lysed, and the fusion protein was purified using glutathione-agarose resin (Sigma-Aldrich) following the manufacturer's instructions. The fusion protein was cleaved with PreScission protease to remove the GST tag. A stationary culture containing pET16b-RalB was diluted 1:10 into 2TY, grown to an  $A_{600}$  of  $\sim$ 0.8 at 37 °C, induced with 1 mM IPTG, and grown for a further 3 h at 37 °C. Cells were lysed, and the fusion protein was purified using Ni-NTA resin (Qiagen) as described above. The fusion protein was cleaved with Factor Xa (Roche) to remove the His tag. A stationary culture containing pMAT10P-full-length RalB was diluted 1:10 into 2TY, grown to an  $A_{600}$  of  $\sim$ 0.8 at 37 °C, induced with 1 mM IPTG, and grown for a further 16 h at 20 °C. Cells were lysed, and the fusion protein was purified using Ni-NTA resin (Qiagen) as described above. The fusion protein was cleaved with PreScission protease to remove the His-MBP tag. All Ral proteins were further purified by gel filtration (S75 16/60, GE Healthcare).

A stationary culture of each RLIP76 RBD construct was diluted 1:10 into 2TY, grown to an  $A_{600}$  of  $\sim$ 0.8 at 37 °C, induced with 0.1 mM IPTG, and grown for a further 5 h at 37 °C. Cells were lysed, and the fusion protein was purified using glutathione agarose (Sigma-Aldrich) following the manufacturer's instructions. The fusion protein was cleaved with thrombin to remove the GST tag and further purified by gel filtration (S30 16/60, GE Healthcare). An accurate concentration of each protein was determined using amino acid analysis by the Protein and Nucleic Acid Chemistry Facility of the Department of Biochemistry of the University of Cambridge. This protein was then used directly in SPAs. Purification of the Sec5 RBD has been described previously.<sup>22</sup>

**Mutagenesis of the RLIP76 RBD.** Mutations were introduced, as specified, into the coding region of the RLIP76 RBD using the QuikChange Lightning Multi Site Directed Mutagenesis Kit (Agilent) following the manufacturer's instructions. The sequences of the coding regions of all mutants were verified by the DNA Sequencing Facility of the Department of Biochemistry of the University of Cambridge.

**Nucleotide Exchange.** Ral proteins were labeled with [ $^3\text{H}$ ]GTP for use in binding assays as described previously.<sup>22</sup>

**Scintillation Proximity Assays (SPA).** Affinities of Ral proteins for the RLIP76 RBD-His domain and its variants were measured using SPA. RLIP76 RBD-His variants (80 nM) were immobilized on Protein A SPA fluoromicrospheres via an anti-His antibody (Sigma-Aldrich). GST-Sec5 (20 nM) was immobilized via an anti-GST antibody as described previously.<sup>22</sup> The equilibrium binding constants ( $K_d$ ) of the effector–G protein interaction were determined by monitoring the SPA signal in the presence of varying concentrations of [ $^3\text{H}$ ]GTP–Ral, as described previously.<sup>23</sup> Binding of Ral to the effector protein brings the radiolabeled nucleotide sufficiently close to the scintillant to obtain a signal. For each Ral protein, an experiment was performed in the absence of effector, which resulted in a linear increase in background SPA counts. This data set was then subtracted from the data points obtained in the presence of effector and plotted as a function of increasing Ral protein concentration. For each affinity determination, data points were obtained for at least 10 different G protein concentrations. Binding curves were fitted using a direct binding isotherm<sup>23</sup> to obtain  $K_d$  values and their standard errors for the G protein–effector interactions.

## RESULTS

### Binding Affinity of the RLIP76 RBD for Ral Isoforms.

Previously, we had measured the affinity of the RLIP76 RBD for both RalA and RalB and found that the two Ral isoforms interacted with similar affinities (our unpublished data and ref 20). We described a similar situation with another Ral effector, Sec5.<sup>22</sup> For practical reasons, these measurements had been undertaken with RalA 1–206 (full-length) and RalB 1–185 (C-terminal truncation). This prompted us to investigate the binding affinities of full-length and truncated RalA and truncated RalB for the RLIP76 RBD, along with the RBD of a second Ral effector, Sec5, for comparison. The apparent  $K_d$  values for the interaction between the Ral variants and the RLIP76 RBD were determined by SPA. The binding isotherms are shown in Figure 1, and the affinities are summarized in Table 1. Full-length RalA binds RLIP76 RBD with a  $K_d$  of  $324 \pm 22$  nM, while RalA  $\Delta$ C binds with a  $K_d$  of  $264 \pm 16$  nM. RalB  $\Delta$ C binds with a  $K_d$  of  $209 \pm 14$  nM. Despite repeated attempts, we were unable to purify sufficiently high quality full-length RalB to perform equivalent experiments with this variant. Full-length RalA binds Sec5 RBD with a  $K_d$  of  $121 \pm 13$  nM, while RalA  $\Delta$ C binds with a  $K_d$  of  $192 \pm 15$  nM. RalB  $\Delta$ C binds with a  $K_d$  of  $135 \pm 9$  nM.

The C-terminal tail of the Ral proteins, as with most small G proteins, is thought to direct membrane localization in the cell. As such, it is usually unavailable for effector binding, although we have previously identified a role for the C-terminal polybasic region from one small G protein (Rac1) in effector binding.<sup>24</sup> These data indicate that full-length RalA and RalA  $\Delta$ C bind with equivalent affinity to RLIP76 and Sec5. RalA  $\Delta$ C and RalB  $\Delta$ C also bind with similar affinities to each effector protein. We decided to proceed with a comparative study of binding of RalA  $\Delta$ C and RalB  $\Delta$ C to RLIP76 to look for thermodynamic differences in the two Ral–RLIP76 complexes.

**Thermodynamic Mapping of the RLIP76 and Sec5 Binding Surfaces on RalB.** The structures of Ral proteins in complex with the RLIP76 and Sec5 Ral binding domains<sup>25,26</sup> provided the starting points for mapping the energetics of the

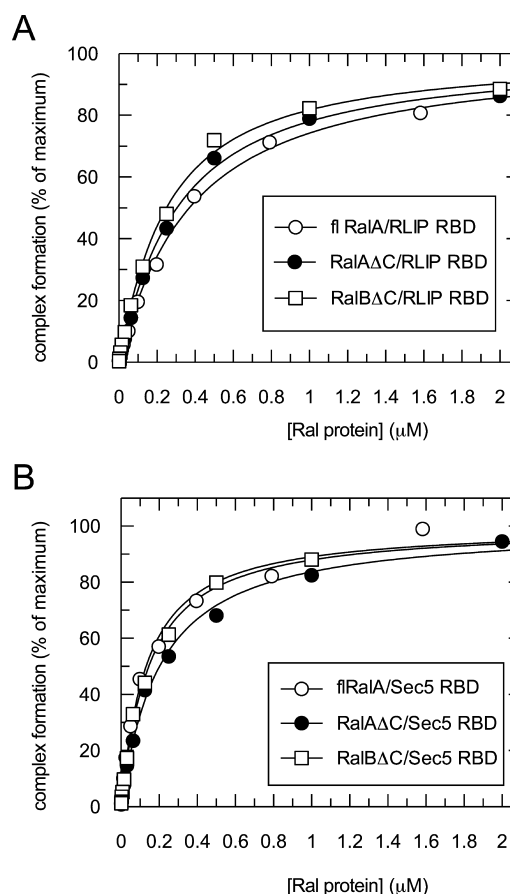


**Figure 1.** SPA binding data for full-length RalA, truncated RalA, and truncated RalB with the RLIP76 RBD and the Sec5 RBD. The indicated concentration of [ $^3\text{H}$ ]GTP-labeled G protein was incubated with either His-tagged RLIP76 RBD or GST-tagged Sec5 RBD, as appropriate, in each SPA. The SPA signal was corrected by subtraction of the background signal from parallel measurements in which the effector protein was omitted. The effect of the concentration of G protein on this corrected SPA signal was fitted to a binding isotherm to give an apparent  $K_d$  value and the signal at saturating G protein concentrations. The data and curve fits are displayed as a percentage of this maximal signal: (A) binding isotherms of full-length and truncated RalA and truncated RalB with the RLIP76 RBD and (B) binding isotherms of full-length and truncated RalA and truncated RalB with the Sec5 RBD.

**Table 1.** Affinities of Ral Variants for RLIP76 and Sec5 RBDs

	apparent $K_d$ (nM) <sup>a</sup>	
	RLIP76 RBD	Sec5 RBD
fl RalA, Q72L	$324 \pm 22$	$121 \pm 13$
RalA $\Delta$ C, Q72L	$264 \pm 16$	$192 \pm 15$
RalB $\Delta$ C, Q72L	$209 \pm 14$	$135 \pm 9$

<sup>a</sup>Equilibrium binding constants were determined in SPAs as described in Methods.  $K_d$  values are quoted with the standard errors from curve fitting.

interface between RalB and these effectors. We analyzed the interfaces of the complexes [Protein Data Bank (PDB) entries 1UAD and 2KWI] to identify residues on the small G protein that were within 4 Å of an effector residue and mutated these to alanine in RalB. There are two side chains in RalB that interact with these effectors that are already alanine: Ala48 and Ala77. Ala48 contacts both RLIP76 and Sec5 and was changed to Gly,



so that the requirement for the alanine methyl group could be probed. Ala48 lies within switch 1, which is unstructured and highly flexible in active RalB, so substitution with a glycine is unlikely to affect the secondary structure. Ala77 is within a helix in switch 2 in RalB and interacts with His413 and various hydrophobic residues in RLIP76. We therefore mutated it to a larger, charged residue (Arg). Other mutations were also made as follows. Tyr36 forms a hydrogen bond in both Sec5 and RLIP76 complexes, so we mutated it to Phe, reasoning that this would remove the hydroxyl group while maintaining the bulky aromatic ring. Glu38 forms a salt bridge with Arg27 in the Sec5 complex, so we mutated it to Gln, hence removing the charge but maintaining the size of the side chain. Two mutations were made to Thr46, although this residue does not interact directly with either effector. Thr46 is equivalent to Ras Thr35, whose mutation to Ser prevented binding of Ras to RalGDS and PI3K but not to Raf.<sup>27,28</sup> The T46S mutant is the direct equivalent and was tested to investigate whether this mutation would discriminate between RLIP76 and Sec5. The T46A mutation was also generated, to study the effect of removing the hydroxyl group completely. Finally, the D49E mutation was generated because this is mutant is known to prevent binding to Sec5 but not to RLIP76 in yeast two-hybrid experiments.<sup>29</sup> This therefore allowed an assessment of whether the *in vitro* affinity measurements correlate with the effects of this mutation in a (yeast) cell.

The apparent  $K_d$  values for the interaction between the RalB mutants and the RLIP76 and Sec5 RBDs were determined by SPA. Selected binding isotherms are shown in panels A and B of Figure 2, and the affinities are summarized in Table 2.

Mutations that reduce binding between the RLIP76 RBD and RalB include Y36A, T46A, T46S, D49A, Y51A, L67A, Y82A, and R84A, which decrease the affinity >10-fold; E38A and E73A, which decrease the affinity between 5- and 10-fold; and E38Q, A48G, R52A, I78A, and N81A, which all decrease the affinity between 3- and 5-fold. Interestingly one mutation, S50A, shows a small increase in binding affinity for RLIP76. Thus, Tyr36, Thr46, Asp49, Tyr51, Leu67, Glu73, Tyr82, and Arg84 all contribute at least 1.2 kcal/mol to the interface, with Tyr51 and Tyr82 making the largest individual contributions.

Mutations Y36A/F, E38A/Q, T46A/S, D49E, and Y51A all effectively abrogate binding to Sec5, and mutations L14A, K47A, and L67A all decrease the affinity for Sec5 between 3- and 7-fold. Mutations at other residues show only a minor effect or no change in the binding affinity. Mutation D49A shows a small increase in binding affinity for Sec5.

**Thermodynamic Mapping of the RalA and RalB Binding Surfaces on the RLIP76 RBD.** Having investigated the differences in thermodynamics between a Ral protein and two of its effector proteins, we next wanted to extend our studies to see if there were any differences in the energetic contributions of an effector protein for the two Ral proteins. RalA and RalB have 82% sequence identity but are 100% identical across the residues that contact RLIP76,<sup>20</sup> so we next investigated the energetic contributions of side chains on the RLIP76 RBD to binding to the Ral small G proteins. In a manner similar to our dissection of the RalB interaction surface, we identified side chains of RLIP76 residues that were within 4 Å of a RalB side chain in our RalB–RLIP76 RBD structure and mutated them to alanine. The apparent  $K_d$  values for the interaction between the RLIP76 RBD mutants and RalB were determined by SPA. Selected binding isotherms are shown in Figure 3A, and the affinities are summarized in Table 3.

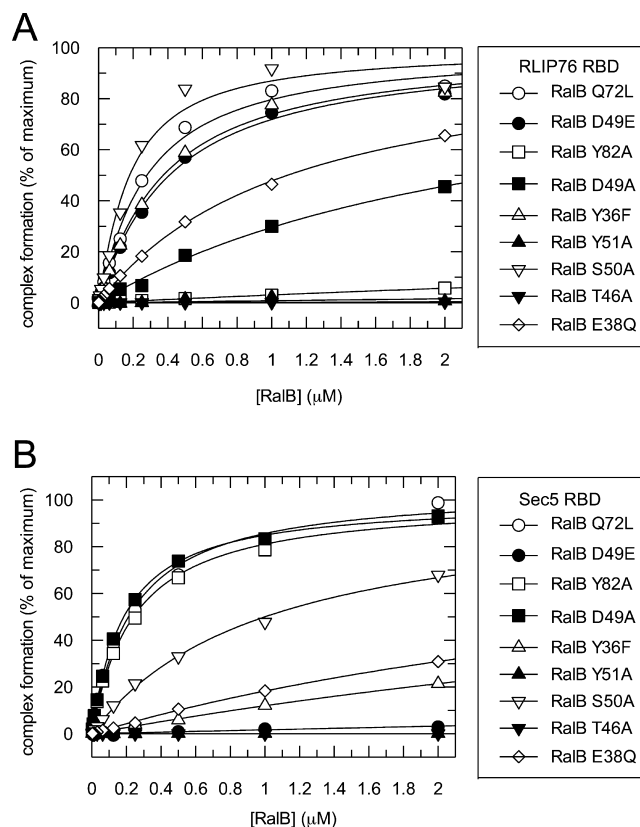


**Figure 2.** SPA binding data for truncated RalB and mutant variants with the RLIP76 RBD and the Sec5 RBD. The indicated concentration of [<sup>3</sup>H]GTP-labeled G protein was incubated with either His-tagged RLIP76 RBD or GST-tagged Sec5 RBD, as appropriate, in each SPA. The SPA signal was corrected by subtraction of the background signal from parallel measurements in which the effector protein was omitted. The effect of the concentration of G protein on this corrected SPA signal was fitted to a binding isotherm to give an apparent  $K_d$  value and the signal at saturating G protein concentrations. The data and curve fits are displayed as a percentage of this maximal signal: (A) binding isotherms of truncated RalB and mutants with the RLIP76 RBD and (B) binding isotherms of truncated RalB and mutants with the Sec5 RBD.

Substitution of RLIP76 residues His413, Trp430, and Thr437 with alanine ablated the binding to RalB; substitutions of Leu409, Leu429, and Lys440 with alanine reduced the affinity significantly (16.5-, 22.8-, and 8.8-fold, respectively), and substitution of Leu416 with alanine reduced the affinity 4.7-fold. Mutations at the remaining residues tested had deleterious effects on RalB binding but to a lesser extent and were thus considered to be individually insignificant, with one exception. Introducing the Q417A mutation into the RLIP76 RBD enhanced binding to RalB by >2-fold.

We then tested the same panel of RLIP76 RBD mutants for their ability to bind RalA. Selected binding isotherms are shown in Figure 3B, and the affinities are summarized in Table 3. Similar to the case for RalB, mutation of residues Leu409, His413, Trp430, Thr437, and Lys440 to alanine all decrease the level binding by ~9-fold or more. Mutation of residue Leu416 decreased the affinity 9-fold, which is larger than the reduction in affinity for RalB for this mutation, while mutation of Leu429 reduced the affinity by 5.6-fold, significantly less than the effect on RalB affinity. Mutating Arg434 to alanine abrogated binding to RalA but had very little effect (2–3-fold reduction) on RalB.

Table 2. Affinities of RalB Mutants for the RLIP76 RBD and Sec5 RBD

RalB	RLIP76				Sec5			
	$K_d$ (nM) <sup>a</sup>	$\Delta G$ (cal/mol)	$\Delta\Delta G$ (cal/mol)	$\alpha$ -fold change	$K_d$ (nM)	$\Delta G$ (cal/mol)	$\Delta\Delta G$ (cal/mol)	$\alpha$ -fold change
Q72L (wt)	216 ± 19	−9088	—	—	238 ± 15	−9030	—	—
L14A,Q72L	300 ± 32	−8893	−195	1.4 ↑	1590 ± 112	−7906	−1124	6.7 ↑
Y36A,Q72L	3040 ± 91	−7522	−1371	10.1 ↑	NB <sup>c</sup>			>50 ↑
Y36F,Q72L	335 ± 28	−8828	−260	1.5 ↑	7300 ± 1600	−7003	−2027	30.7 ↑
E38A,Q72L	1390 ± 112 <sup>b</sup>	−7986	−1102	6.4 ↑	NB <sup>c</sup>			>50 ↑
E38Q,Q72L	1050 ± 50.1	−8152	−936	4.9 ↑	4460 ± 506	−7295	−1735	18.7 ↑
T46A,Q72L	NB <sup>c</sup>			>50 ↑	NB <sup>c</sup>			>50 ↑
T46S,Q72L	4130 ± 283	−7340	−1553	13.8 ↑	NB <sup>c</sup>			>50 ↑
K47A,Q72L	339 ± 35	−8821	−267	1.6 ↑	763 ± 35	−8341	−689	3.2 ↑
A48G,Q72L	945 ± 61	−8214	−874	4.4 ↑	297 ± 18	−8899	−131	1.2 ↑
D49A,Q72L	2330 ± 349	−7680	−1353	10.8 ↑	175 ± 5	−9213	+183	0.7 ↓
D49E,Q72L	369 ± 25	−8771	−317	1.7 ↑	NB <sup>c</sup>			>50 ↑
S50A,Q72L	140 ± 29	−9345	+257	0.6 ↓	990 ± 79	−8186	−844	4.2 ↑
Y51A,Q72L	NB <sup>c</sup>			>50 ↑	NB <sup>c</sup>			>50 ↑
R52A,Q72L	682 ± 112	−8407	−681	3.2 ↑	371 ± 20	−8768	−262	1.6 ↑
L67A,Q72L	2680 ± 141	−7597	−1491	10.3 ↑	1040 ± 120	−8157	−873	4.4 ↑
E73A,Q72L	1090 ± 127	−8129	−959	5.0 ↑	697 ± 35	−8394	−636	2.9 ↑
D74A,Q72L	326 ± 34	−8844	−244	1.6 ↑	311 ± 11	−8872	−158	1.3 ↑
Y75A,Q72L	544 ± 15	−8541	−547	2.5 ↑	413 ± 35	−8704	−326	1.7 ↑
A77R,Q72L	585 ± 50	−8498	−590	2.7 ↑	203 ± 11	−9125	+95	—
I78A,Q72L	724 ± 55	−8372	−716	3.4 ↑	206 ± 11	−9116	+86	—
N81A,Q72L	696 ± 52	−8395	−693	3.2 ↑	491 ± 48	−8602	−428	2.1 ↑
Y82A,Q72L	12080 ± 3300	−3377	−5711	55 ↑	230 ± 18	−9051	+21	—
R84A,Q72L	2320 ± 89	−7682	−1496	10.7 ↑	501 ± 21	−8590	−440	2.1 ↑

<sup>a</sup>Equilibrium binding constants were determined in SPAs as described in Methods.  $K_d$  values are quoted with the standard errors from curve fitting.

<sup>b</sup> $K_d$  values of >1000 nM (1  $\mu$ M) are based on data for which it was not possible to achieve sufficiently high concentrations to obtain a full binding curve. As such,  $K_d$  values are subject to errors. <sup>c</sup>NB (no binding) denotes data that could not be fit to the binding isotherm.

The remaining residues, when mutated, all had a small detrimental effect on binding to RalA and were not considered to be significant, except Q433A, which had no effect on RalA binding. There were no mutations that increased the level of binding of RalA.

Residues Leu409, His413, Leu429, Trp430, Thr437, and Lys440 all contribute >1.2 kcal/mol to the RLIP76–RalB interface. Residues Leu409, His413, Leu416, Tyr430, Arg434, Thr437, and Lys440 of RLIP76 all contribute >1.2 kcal/mol to the RLIP76–RalA interface.

## DISCUSSION

Using our structure of RalB bound to the RLIP76 RBD<sup>20</sup> and the structure of RalA bound to Sec5,<sup>26</sup> we have designed mutations to probe the thermodynamics of the binding interfaces and dissect the energetic contributions of specific RalB residues for these two effector proteins. Panels A and B of Figure 4 show heat maps for the RLIP76 and Sec5 binding surfaces, respectively, on RalB. It is immediately striking that the energetically important binding surface for RLIP76 is much more extensive than that for Sec5. This is not surprising, because a comparison of the Ral complex structures reveals that the effectors themselves are strikingly different, as are the regions that they contact on the Ral proteins (Figure 4C,D). The Sec5 RBD has an all- $\beta$  sheet, Ig-like fold, which forms an intermolecular antiparallel  $\beta$  sheet with the  $\beta$ 2 strand of RalA, interacting exclusively with residues in and around switch 1 and burying  $\sim$ 1000 Å<sup>2</sup> in the interface.<sup>26</sup> The RLIP76 RBD–RalB structure<sup>20</sup> shows that the RLIP76 RBD forms a simple coiled coil, which interacts with both switch 1 and switch 2 in RalB and buries  $\sim$ 1700 Å<sup>2</sup>. It is logical, therefore, that we find residues

with significant energetic input into RalB–RLIP76 complex formation across RalB switches 1 and 2. For Sec5, the largest energetic contributions are exclusively found from residues in switch 1 of RalB. These thermodynamic differences highlight certain RalB residues that if mutated would differentially discriminate between effectors. For example, RalB Y82A or D49A mutants would no longer bind to RLIP76 but would retain the ability to bind to Sec5. Conversely, RalB Y36F or D49E should retain the ability to bind RLIP76 but no longer be competent to bind Sec5. Such mutations should be useful tools for dissecting Ral effector pathways *in vivo*. In fact, the affinities of the D49E mutant that we have quantified *in vitro* are in agreement with the results found for this mutation by a yeast two-hybrid experiment and by co-immunoprecipitation in HEK293T cells.<sup>29</sup> Thus, all of the mutants that we describe here are likely to have the same effects *in vivo* as we have seen *in vitro*.

Some of the residues whose mutation affects binding are not involved in directly contacting the effector but play a supporting role in maintaining the structure of the RalB interacting residues. For example, in both complexes, Thr46 makes no direct contact with the effectors (Figure 4C,D), but its mutation to Ser or Ala significantly reduces binding to both. As this Thr residue contacts the Mg<sup>2+</sup> ion in the RalB protein, it is not surprising that the integrity of the switch regions is compromised. The T46A/S mutants can still, however, be loaded with the GTP analogue, and T46S shows some affinity for RLIP76. Similarly, Leu67, which is close to the interface in both complexes, forms hydrophobic contacts in RLIP76 but not in Sec5. In the latter, it still has a small effect on binding, presumably because it supports the RalB  $\beta$ 2 strand, which is involved in an intermolecular

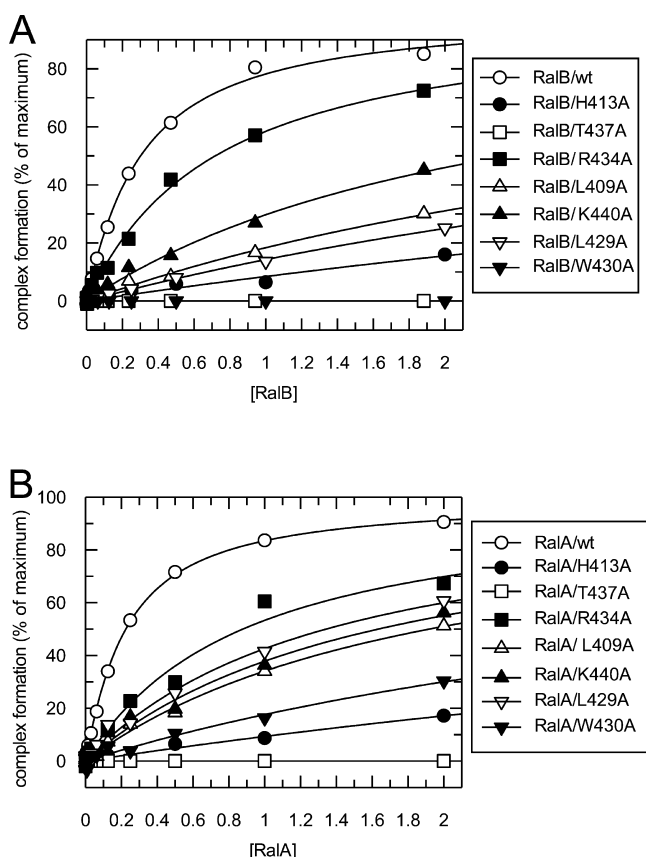


**Figure 3.** SPA binding data for the RLIP RBD and mutant variants with truncated RalA and RalB. The indicated concentration of [<sup>3</sup>H]GTP-labeled G protein was incubated with the appropriate His-tagged RLIP76 RBD variant in each SPA. The SPA signal was corrected by subtraction of the background signal from parallel measurements in which the effector protein was omitted. The effect of the concentration of G protein on this corrected SPA signal was fitted to a binding isotherm to give an apparent  $K_d$  value and the signal at saturating G protein concentrations. The data and curve fits are displayed as a percentage of this maximal signal: (A) binding isotherms of the RLIP76 RBD variants with truncated RalB and (B) binding isotherms of the RLIP76 RBD variants with truncated RalA.

$\beta$  sheet with Sec5 (Figure 4D). This is also the case for Leu14, which is within  $\beta$ 1 and packs next to Leu67. Leu14 reduces Sec5 binding but not RLIP76 binding, highlighting the importance of the intermolecular  $\beta$ -sheet in the Sec5 interaction. There are also supporting residues in the RalB–RLIP76 interaction whose mutations affect binding. The E38A mutant knocks out Sec5 binding and reduces RLIP76 binding. In the Sec5 complex, Glu38 forms a salt bridge with Sec5 residue Arg27 but Glu38 does not contact RLIP76 directly. Instead, it is likely to be involved in maintaining the position of the neighboring residue, Tyr36, which does contact RLIP76. It is possible that replacing the charged Glu38 with the smaller, hydrophobic Ala allows the  $\alpha$ 1 helix to be extended to residue 38, altering its conformation and that of switch 1. This is consistent with the observation that the E38Q mutation has a lesser effect on the binding of RLIP76, since Gln38 is not charged but is more polar than Ala. A similar argument may explain the effect of the E73A mutant, which reduces binding of RLIP76 5-fold. Glu73 is next to the switch 2 helix,  $\alpha$ 2, and its mutation to Ala is likely to alter  $\alpha$ 2 and therefore the ability of residues in this helix to contact RLIP76.

Some of the mutations that we have tested here have previously been generated in RalA and their effects on Exo84 and Sec5 measured.<sup>30</sup> The effects on Sec5 binding were broadly consistent with our observations on the RalB–Sec5 interaction; for example, the E38A mutation did not affect Exo84 binding but reduced the affinity for Sec5 ~45-fold just as in RalB (Table 1). The R52A mutant of RalA bound to Sec5, with an affinity similar to that of the wild type, similar to its effects in RalB, but reduced the affinity of Exo84 18-fold. Arg52 forms a hydrogen bond in the RalA–Exo84 complex, so the effects of this mutation can be explained.

We next resolved the contribution of RLIP76 residues to complex formation with RalA and RalB. Panels A and B of Figure 5 show the energetically important residues on RLIP76 for RalA and RalB binding. It is striking that although the residues in RalB that contact RLIP76 are 100% conserved in RalA, the binding hot spots on RLIP76 are not identical (Table 3): removal of the Leu412 side chain has a weak effect on RalA binding but does not change RalB binding; the L429A mutation

**Table 3. Affinities of RLIP76 RBD Mutants for Ral Isoforms<sup>a</sup>**

RLIP76 RBD	RalA				RalB			
	$K_d$ (nM)	$\Delta G$ (cal/mol)	$\Delta\Delta G$ (cal/mol)	$\alpha$ -fold change	$K_d$ (nM)	$\Delta G$ (cal/mol)	$\Delta\Delta G$ (cal/mol)	$\alpha$ -fold change
C411S (wt)	185 ± 5	−9180	—	—	261 ± 17	−8976	—	—
L409A,C411S	1880 ± 297 <sup>b</sup>	−7807	−1373	10.0 ↑	4300 ± 1400	−7317	−1659	16.5 ↑
L412A,C411S	774 ± 123	−8332	−848	4.2 ↑	228 ± 24	−9056	—	—
H413A,C411S	NB <sup>c</sup>	—	—	>69 ↑	NB <sup>c</sup>	—	—	>16 ↑
L416A,C411S	1700 ± 309	−7866	−1314	9.2 ↑	1240 ± 147	−8053	−923	4.7 ↑
Q417A,C411S	126 ± 27	−9407	—	—	99 ± 22	−9550	+574	2.2 ↓
K421A,C411S	433 ± 37	−8676	−504	2.3 ↑	441 ± 30	−8665	−311	0.6 ↑
E426A,C411S	437 ± 131	−8671	−509	2.4 ↑	670 ± 33	−8418	−558	2.6 ↑
E427A,C411S	452 ± 45	−8651	−529	2.4 ↑	618 ± 39	−8465	−511	2.4 ↑
L429A,C411S	1030 ± 308	−8163	−1017	5.6 ↑	5940 ± 928	−3588	−5388	22.8 ↑
W430A,C411S	NB <sup>c</sup>	—	—	>69 ↑	NB <sup>c</sup>	—	—	>16 ↑
Q433A,C411S	216 ± 43	−9088	—	—	197 ± 20	−9142	—	—
R434A,C411S	NB <sup>c</sup>	—	—	>69 ↑	678 ± 77	−8411	−565	2.6 ↑
T437A,C411S	NB <sup>c</sup>	—	—	>69 ↑	NB <sup>c</sup>	—	—	>16 ↑
K440A,C411S	1590 ± 410	−7906	−1274	8.6 ↑	2300 ± 450	−7687	−1289	8.8 ↑

<sup>a</sup>Equilibrium binding constants were determined in SPAs as described in Methods.  $K_d$  values are quoted with the standard errors from curve fitting.

<sup>b</sup> $K_d$  values of >1000 nM (1  $\mu$ M) are based on data where it was not possible to achieve sufficiently high concentrations to obtain a full binding curve. As such,  $K_d$  values are subject to errors. <sup>c</sup>NB (no binding) denotes data that could not be fit to the binding isotherm.



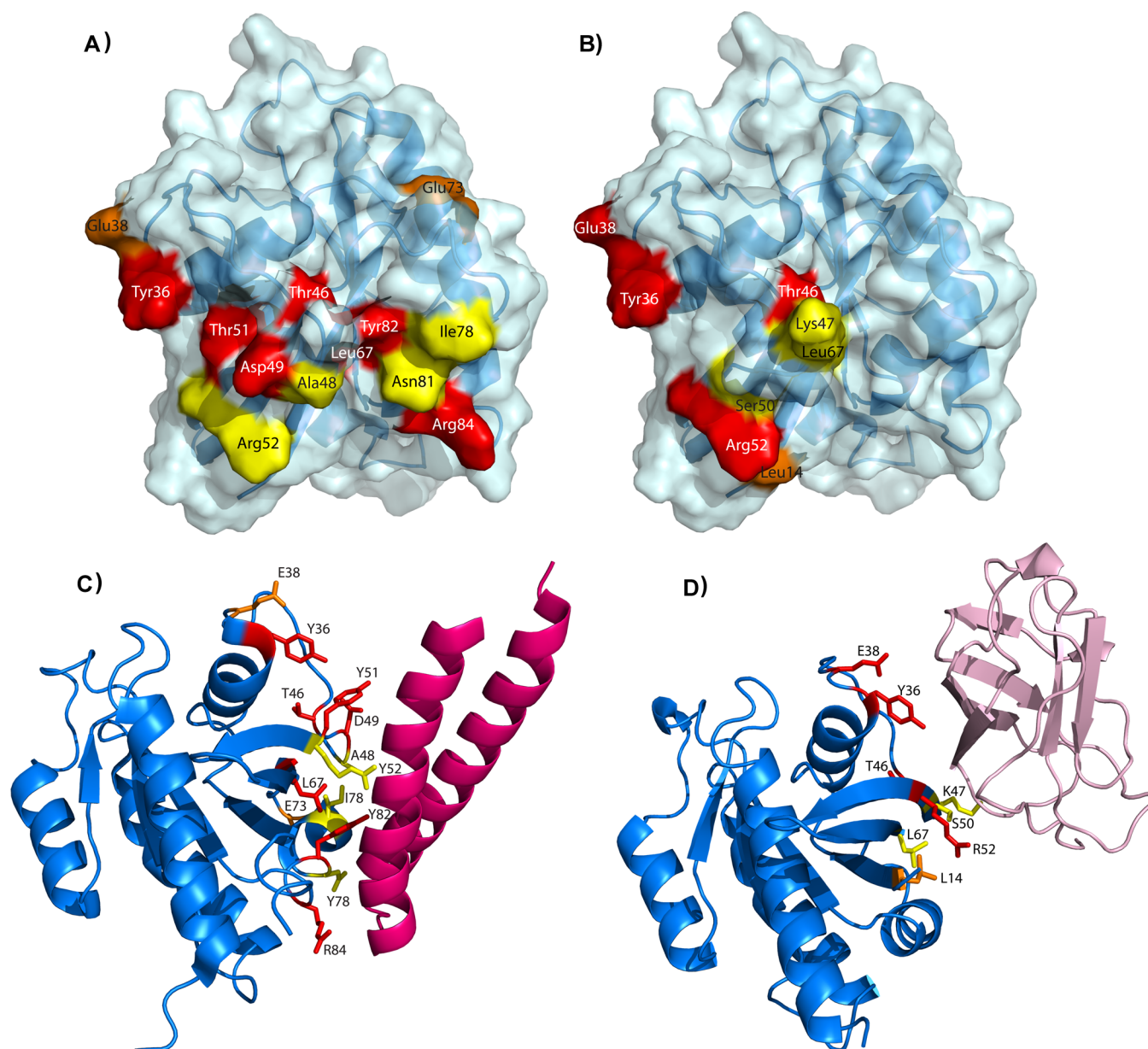


**Figure 4.** Structural details of the RalB–RLIP76 and RalB–Sec5 interfaces. (A) Residues whose mutation to Ala affects binding to RLIP76. RalB is shown as a blue ribbon, overlaid with a semitransparent blue surface. Relevant residues are colored as follows: red, >10-fold weaker affinity; orange, 5–10-fold weaker affinity; yellow, 3–5-fold weaker affinity. Switch 1 encompasses residues 40–50 and switch 2 residues 70–84, as assigned by comparing the structures in PDB entries 1U8Y and 1U90.<sup>37</sup> (B) Residues whose mutation to Ala affects binding to Sec5. The colors are the same as in panel A. (C) Structure of the RalB–RLIP76 complex (PDB entry 2KWI) shown with the residues whose mutation affects RLIP binding shown as sticks. RalB is colored blue and RLIP76 dark pink. The mutated residues are shown in the same color scheme as in panel A. (D) Model of the RalB–Sec5 complex, constructed using Modeler<sup>38</sup> based on PDB entry 1UAD, with the residues that affect Sec5 binding shown as sticks. RalB is colored blue and Sec5 pale pink. The mutated residues are shown in the same color scheme as in panel A.

reduces RalA binding <6-fold but has a more significant effect on RalB binding (23-fold); and R434A in the RLIP76 RBD abrogates binding to RalA completely, while binding to RalB is not significantly affected (<3-fold).

Leu412 does not directly contact RalB and instead is packed within the RLIP76 coiled coil directly behind Leu429. It is therefore likely that the effects of the L412A mutation are mediated via small changes in the orientation of the helices of the coiled coil, which in turn lead to subtle rearrangements of the side chains that do interact with the RalA molecule. Replacement of Leu412 with the smaller Ala side chain would create a cavity inside the coiled coil unless the two helices shift

closer together. Such a shift would move one of the helices further away from the Ral molecule.

Leu429 contacts three residues in RalB switch 2, Ala77, Asn81, and Tyr82, all of which are conserved in RalA. Arg434 makes contacts with Lys16 and Asp65, which again are conserved in RalA. Indeed, a comparison of all of the differences in sequence between the truncated versions of RalA and RalB that were used in this study shows that all of the changes are away from the switch regions and the RLIP76 binding site (Figure 5C). The most dramatic difference between RalA and RalB lies in the insertion of Ala116 in the loop between helix  $\alpha 3$  and strand  $\beta 5$ . The same loop is also modified by the

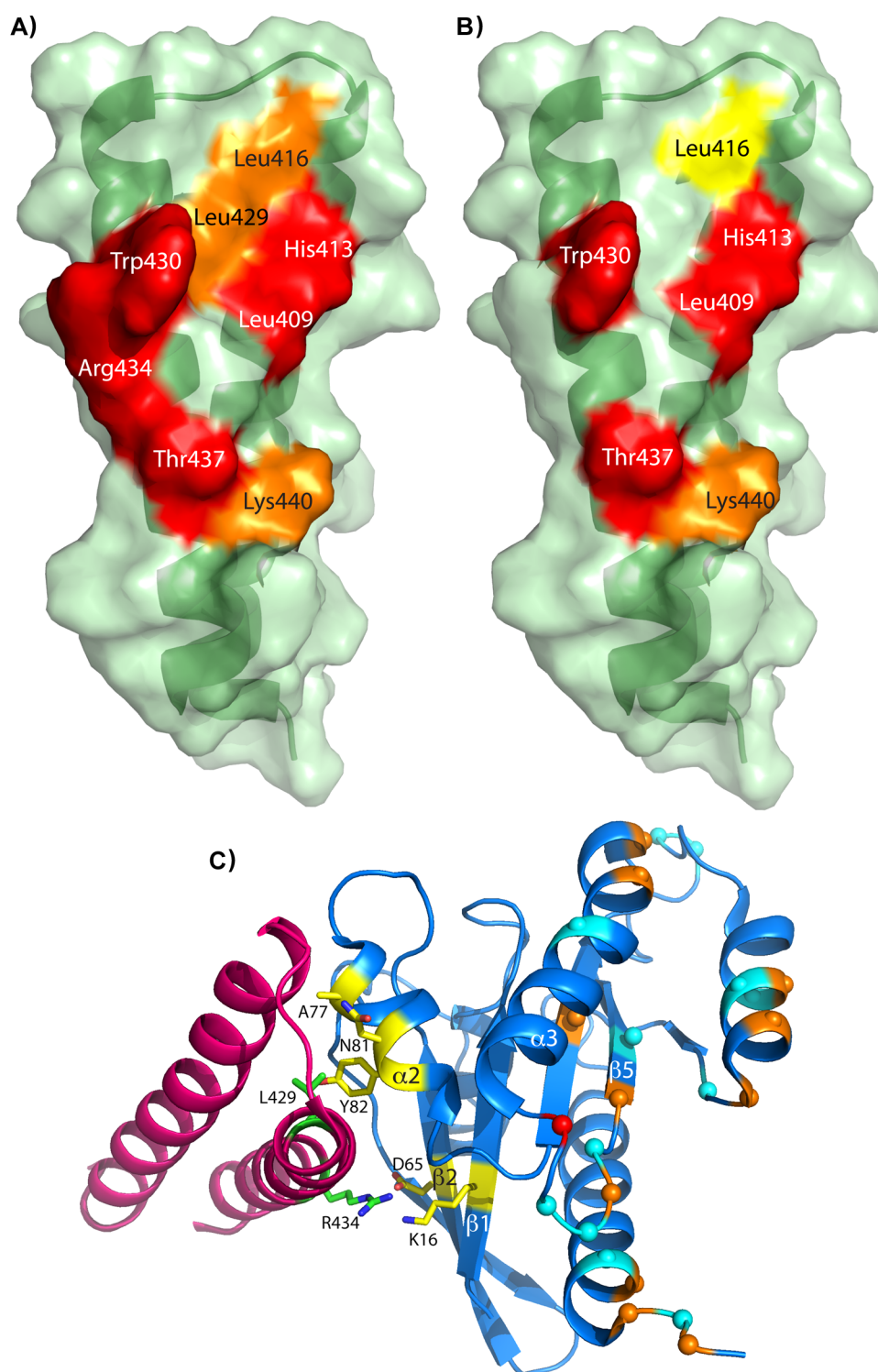


**Figure 5.** Hot spots on RLIP76 for binding to Ral proteins. (A) Residues whose mutation to Ala disrupts binding to RalA. Relevant residues are colored as follows: red, >10-fold weaker affinity; orange, 5–10-fold weaker affinity; yellow, 3–5-fold weaker affinity. (B) Residues whose mutation to Ala disrupts binding to RalB. The color scheme for residues is the same as in panel A. (C) Two residues whose mutation has drastically different effects on binding of RalA and RalB to RLIP76. RalB is colored blue and RLIP76 dark pink. Leu429 and Arg434 are colored green, and the residues that they contact in RalB are colored yellow. The positions of conservative changes between RalA and RalB are shown as cyan spheres: these include Asp/Glu, Lys/Arg, Val/Ile/Leu, or Asn/Gln exchanges only. The positions of less conservative changes between the two proteins are shown as orange spheres. Finally, the position of a single amino acid insertion (Ala116) in RalB is shown as a red sphere.

substitution of the neutral Asn119 in RalA with Lys120 in RalB. These changes lead to a different conformation in this loop when RalA and RalB are compared. In both Ral proteins, this loop is mobile, exhibiting high temperature factors in the X-ray

structures of RalA and dynamics on a picosecond to nanosecond time scale in RalB.<sup>22</sup> The insertion in the loop is likely to cause a subtle shift in the position of the C-terminus of helix  $\alpha 3$ , which is in direct contact with helix  $\alpha 2$  at the C-terminus of



switch 2 (Figure 5C). Any changes in switch 2 would also be readily transmitted to strands  $\beta 1$  and  $\beta 2$ , which lie underneath switch 2. Hence, the changes in the  $\alpha 3$ – $\beta 5$  loop sequence and length may be responsible for the differences in the contribution of residues in switch 2 (Ala77, Asn81, and Tyr82) and strands  $\beta 1$  and  $\beta 2$  (Lys16 and Asp65) to interactions with RLIP76 Leu429 and Arg434. For the purposes of this discussion, we have assumed that Leu429 and Arg434 contact broadly the same residues in RalA as in RalB, which is likely although not certain in the absence of a RalA–RLIP76 structure.

Interestingly, substitution of one residue, Gln417, with Ala had little effect on RalA binding but slightly increased (2.2-fold) the affinity of the RalB complex. This residue also contacts RalB switch 2, via the side chain of Tyr75. The effects of this mutation therefore also support the idea that switch 2 is subtly different in the RalA and RalB isoforms. This is in agreement with our nuclear magnetic resonance (NMR) analysis, which suggests that switch 2 has some differences in millisecond time scale dynamics in the two Ral proteins (manuscript in preparation).

A number of the mutations that we have identified are likely to mediate their effects on binding via medium-range structural rearrangements. Allostery in GTPases has been observed in several situations, and its exploitation is becoming increasingly important for targeting these proteins. Binding of calcium acetate to helix 3–loop 7 of Ha-Ras, in a crystallized form, results in structural rearrangements that ultimately order the N-terminal region of switch II and position Glu61 in the active site.<sup>31</sup> Identification of a unique pocket in the Ki-Ras G12C oncogenic variant prompted screening for binding compounds. This pocket is adjacent to the nucleotide binding site, and binding compounds that change the nucleotide affinity have been identified, leading to a preference for GDP over GTP and simultaneously block GEF activation using an allosteric mechanism.<sup>32</sup> A region adjacent to but distinct from the nucleotide binding site has also been utilized to target inhibitors to the Ral GTPases. Again, binding to this allosteric site is sufficient to modulate GTPase activity *in vitro* and *in vivo*.<sup>33</sup> Dynamic exchange between different conformations is also well-documented in small G proteins. NMR has shown that Ha-Ras bound to GTP or GTP analogues exhibits dynamics on a millisecond time scale.<sup>34,35</sup> Furthermore, <sup>31</sup>P NMR experiments suggested the presence of multiple conformations in active forms of small GTPases.<sup>22,36</sup> Taken together, these studies demonstrate the importance of conformational and structural flexibility to small G protein function and also establish the utility of this feature as a means of attacking these proteins therapeutically.

In summary, our hot spot analysis of the binding of RLIP76 to RalA and RalB suggests that at least some of the differences in the Ral proteins lie in the structure and dynamics of switch 2 and the consequences for effector binding that ensue. We have identified some residues of RLIP76 that can be mutated to prevent its binding to both RalA and RalB, e.g., His413 and Trp430. Furthermore, we have identified two residues whose mutation will allow discrimination between the Ral isoforms: the L429A mutation will reduce RalB binding significantly more than binding, while the R434A mutation abrogates RalA binding but has little effect on RalB binding. These mutants represent essential tools for dissecting the roles of RalA and RalB *in vivo*.

## AUTHOR INFORMATION

### Corresponding Authors

\*E-mail: do202@cam.ac.uk.

\*E-mail: hrm28@cam.ac.uk.

### Funding

This research was supported by a BBSRC Studentship to M.D.C., a Pakistan HEC and Cambridge Overseas Trust Studentship to A.S., CR-UK Project Grant C9467/A4658 (to D.O. and H.R.M.), and MRC Project Grants G0700057 and MR/J007803/1 (to D.O. and H.R.M.).

## ACKNOWLEDGMENTS

We are grateful to the Captain Stephanos Foundation for support to M.P. during her undergraduate training. We also thank Ms. Joanna Watson for practical guidance to M.P.

### Notes

The authors declare no competing financial interest.

## ABBREVIATIONS

RBD, Ral binding domain; IPTG, isopropyl  $\beta$ -D-1-thiogalactopyranoside; GST, glutathione S-transferase; GTP, guanosine 5'-triphosphate; GDP, guanosine 5'-diphosphate; DTT, dithiothreitol; SPA, scintillation proximity assay.

## REFERENCES

- (1) Cascone, I., Selimoglu, R., Ozdemir, C., Del Nery, E., Yeaman, C., White, M., and Camonis, J. (2008) Distinct roles of RalA and RalB in the progression of cytokinesis are supported by distinct RalGEFs. *EMBO J.* 27, 2375–2387.
- (2) Bodemann, B. O., Orvedahl, A., Cheng, T., Ram, R. R., Ou, Y.-H., Formstecher, E., Maiti, M., Hazelett, C. C., Wauson, E. M., Balakireva, M., Camonis, J. H., Yeaman, C., Levine, B., and White, M. A. (2011) RalB and the Exocyst Mediate the Cellular Starvation Response by Direct Activation of Autophagosome Assembly. *Cell* 144, 253–267.
- (3) Kashatus, D. F., Lim, K.-H., Brady, D. C., Pershing, N. L. K., Cox, A. D., and Counter, C. M. (2011) RalA and RalBP1 regulate mitochondrial fission at mitosis. *Nat. Cell Biol.* 13, 1108–1115.
- (4) Shipitsin, M., and Feig, L. A. (2004) RalA but not RalB enhances polarized delivery of membrane proteins to the basolateral surface of epithelial cells. *Mol. Cell. Biol.* 24, 5746–5756.
- (5) Rosse, C., Hatzoglou, A., Parrini, M. C., White, M. A., Chavrier, P., and Camonis, J. (2006) RalB mobilizes the exocyst to drive cell migration. *Mol. Cell. Biol.* 26, 727.
- (6) Chien, Y. C., and White, M. A. (2003) Ral GTPases are linchpin modulators of human tumour-cell proliferation and survival. *EMBO Rep.* 4, 800.
- (7) Kashatus, D. F. (2013) Ral GTPases in tumorigenesis: Emerging from the shadows. *Exp. Cell Res.* 319, 2337–2342.
- (8) Chardin, P., and Tavitian, A. (1989) Coding Sequences of Human RalA and RalB cDNAs. *Nucleic Acids Res.* 17, 4380–4380.
- (9) Takai, Y., Sasaki, T., and Matozaki, T. (2001) Small GTP-binding proteins. *Physiol. Rev.* 81, 153–208.
- (10) Martin, T. D., Mitin, N., Cox, A. D., Yeh, J. J., and Der, C. J. (2012) Phosphorylation by Protein Kinase Ca Regulates RalB Small GTPase Protein Activation, Subcellular Localization, and Effector Utilization. *J. Biol. Chem.* 287, 14827–14836.
- (11) Jullien-Flores, V., Dorseuil, O., Romero, F., Letourneur, F., Saragosti, S., Berger, R., Tavitian, A., Gacon, G., and Camonis, J. H. (1995) Bridging Ral GTPase to Rho-Pathways: RLIP76, a Ral Effector With Cdc42/Rac GTPase-Activating Protein Activity. *J. Biol. Chem.* 270, 22473–22477.
- (12) Cantor, S. B., Urano, T., and Feig, L. A. (1995) Identification and Characterization of Ral-Binding Protein-1, a Potential Downstream Target of Ral GTPases. *Mol. Cell. Biol.* 15, 4578.

- (13) Park, S. H., and Weinberg, R. A. (1995) A putative effector of Ral has homology to Rho/Rac GTPase activating proteins. *Oncogene* 11, 2349.
- (14) Moskalenko, S., Tong, C., Rosse, C., Mirey, G., Formstecher, E., Daviet, L., Camonis, J., and White, M. A. (2003) Ral GTPases regulate exocyst assembly through dual subunit interactions. *J. Biol. Chem.* 278, 51743–51748.
- (15) Chien, Y. C., Kim, S., Bumeister, R., Loo, Y. M., Kwon, S. W., Johnson, C. L., Balakireva, M. G., Romeo, Y., Kopelovich, L., Gale, M., Yeaman, C., Camonis, J. H., Zhao, Y. M., and White, M. A. (2006) RalB GTPase-mediated activation of the I $\kappa$ B family kinase TBK1 couples innate immune signaling to tumor cell survival. *Cell* 127, 157–170.
- (16) Frankel, P., Aronheim, A., Kavanagh, E., Balda, M. S., Matter, K., Bunney, T. D., and Marshall, C. J. (2005) RalA interacts with ZONAB in a cell density-dependent manner and regulates its transcriptional activity. *EMBO J.* 24, 54.
- (17) Ohta, Y., Suzuki, N., Nakamura, S., Hartwig, J. H., and Stossel, T. P. (1999) The small GTPase RalA targets filamin to induce filopodia. *Proc. Natl. Acad. Sci. U.S.A.* 96, 2122–2128.
- (18) Sidhu, R. S., Clough, R. R., and Bhullar, R. P. (2005) Regulation of phospholipase C- $\alpha$ 1 through direct interactions with the small GTPase Ral and calmodulin. *J. Biol. Chem.* 280, 21933.
- (19) Jiang, H., Luo, J. Q., Urano, T., Frankel, P., Lu, Z. M., Foster, D. A., and Feig, L. A. (1995) Involvement of Ral GTPase in v-Src-Induced Phospholipase-D Activation. *Nature* 378, 409.
- (20) Fenwick, R. B., Campbell, L. J., Rajasekar, K., Prasannan, S., Nietlispach, D., Camonis, J., Owen, D., and Mott, H. R. (2010) The RalB-RLIP76 Complex Reveals a Novel Mode of Ral-Effector Interaction. *Structure* 18, 985–995.
- (21) Strugnell, S. A., Wiefing, B. A., and DeLuca, H. F. (1997) A modified pGEX vector with a C-terminal histidine tag: Recombinant double-tagged protein obtained in greater yield and purity. *Anal. Biochem.* 254, 147–149.
- (22) Fenwick, R. B., Prasannan, S., Campbell, L. J., Nietlispach, D., Evetts, K. A., Camonis, J., Mott, H. R., and Owen, D. (2009) Solution Structure and Dynamics of the Small GTPase RalB in Its Active Conformation: Significance for Effector Protein Binding. *Biochemistry* 48, 2192–2206.
- (23) Graham, D. L., Eccleston, J. F., and Lowe, P. N. (1999) The conserved arginine in Rho-GTPase-activating protein is essential for efficient catalysis but not for complex formation with Rho GDP and aluminum fluoride. *Biochemistry* 38, 985–991.
- (24) Modha, R., Campbell, L. J., Nietlispach, D., Buhecha, H. R., Owen, D., and Mott, H. R. (2008) The Rac1 polybasic region is required for interaction with its effector PRK1. *J. Biol. Chem.* 283, 1492–1500.
- (25) Fenwick, R., Prasannan, S., Campbell, L. J., Evetts, K. A., Nietlispach, D., Owen, D., and Mott, H. R. (2008)  $^1\text{H}$ ,  $^{13}\text{C}$  and  $^{15}\text{N}$  resonance assignments for the active conformation of the small G protein RalB in complex with its effector RLIP76. *Biomol. NMR Assignments* 2, 179–182.
- (26) Fukai, S., Matern, H. T., Jagath, J. R., Scheller, R. H., and Brunger, A. T. (2003) Structural basis of the interaction between RalA and Sec5, a subunit of the sec6/8 complex. *EMBO J.* 22, 3267.
- (27) White, M. A., Nicolette, C., Minden, A., Polverino, A., Van Aelst, L., Karin, M., and Wigler, M. H. (1995) Multiple Ras Functions Can Contribute to Mammalian-Cell Transformation. *Cell* 80, 533–541.
- (28) RodriguezViciano, P., Warne, P. H., Khwaja, A., Marte, B. M., Pappin, D., Das, P., Waterfield, M. D., Ridley, A., and Downward, J. (1997) Role of phosphoinositide 3-OH kinase in cell transformation and control of the actin cytoskeleton by Ras. *Cell* 89, 457–467.
- (29) Moskalenko, S., Henry, D. O., Rosse, C., Mirey, G., Camonis, J. H., and White, M. A. (2002) The exocyst is a Ral effector complex. *Nat. Cell Biol.* 4, 66–72.
- (30) Jin, R. S., Junutula, J. R., Matern, H. T., Ervin, K. E., Scheller, R. H., and Brunger, A. T. (2005) Exo84 and Sec5 are competitive regulatory Sec6/8 effectors to the RalA GTPase. *EMBO J.* 24, 2064.
- (31) Buhrman, G., Holzapfel, G., Fetics, S., and Mattos, C. (2010) Allosteric modulation of Ras positions Q61 for a direct role in catalysis. *Proc. Natl. Acad. Sci. U.S.A.* 107, 4931–4936.
- (32) Ostrem, J. M., Peters, U., Sos, M. L., Wells, J. A., and Shokat, K. M. (2013) K-Ras(G12C) inhibitors allosterically control GTP affinity and effector interactions. *Nature* 503, 548–551.
- (33) Yan, C., Liu, D., Li, L., Wempe, M. F., Guin, S., Khanna, M., Meier, J., Hoffman, B., Owens, C., Wysoczynski, C. L., Nitz, M. D., Knabe, W. E., Ahmed, M., Brautigan, D. L., Paschal, B. M., Schwartz, M. A., Jones, D. N. M., Ross, D., Meroueh, S. O., and Theodorescu, D. (2014) Discovery and characterization of small molecules that target the GTPase Ral. *Nature* 515, 443–447.
- (34) Ito, Y., Yamasaki, K., Iwahara, J., Terada, T., Kamiya, A., Shirouzu, M., Muto, Y., Kawai, G., Yokoyama, S., Laue, E. D., Walchli, M., Shibata, T., Nishimura, S., and Miyazawa, T. (1997) Regional polyesterism in the GTP-bound form of the human c-Ha-Ras protein. *Biochemistry* 36, 9109–9119.
- (35) O'Connor, C., and Kovrig, E. L. (2008) Global conformational dynamics in Ras. *Biochemistry* 47, 10244–10246.
- (36) Geyer, M., Schweins, T., Herrmann, C., Prisner, T., Wittinghofer, A., and Kalbitzer, H. R. (1996) Conformational transitions in p21(ras) and in its complexes with the effector protein Raf-RBD and the GTPase activating protein GAP. *Biochemistry* 35, 10308–10320.
- (37) Nicely, N. I., Kosak, J., de Serrano, V., and Mattos, C. (2004) Crystal structures of Ral-GppNHP and Ral-GDP reveal two binding sites that are also present in Ras and Rap. *Structure* 12, 2025–2036.
- (38) Eswar, N., Webb, B., Marti-Renom, M. A., Madhusudhan, M. S., Eramian, D., Shen, M.-Y., Pieper, U., and Sali, A. (2006) Comparative protein structure modeling using Modeller. *Current protocols in bioinformatics*, Chapter 5, Unit 5.6, Wiley, New York.